HHS Public Access

Author manuscript

J Neurooncol. Author manuscript; available in PMC 2019 April 09.

Published in final edited form as:

J Neurooncol. 2018 September ; 139(2): 293–305. doi:10.1007/s11060-018-2889-2.

"Virus vector-mediated genetic modification of brain tumor stromal cells after intravenous delivery."

Adrienn Volak[1], **Stanley G. LeRoy**[1], **Jeya Shree Natasan**[1], **David J. Park**[1], **Pike See Cheah**[1,5], **Andreas Maus**[1], **Zachary Fitzpatrick**[1], **Eloise Hudry**[1,2], **Kelsey Pinkham**[1], **Sheetal Gandhi**[1,2], **Bradley T. Hyman**[1,2], **Dakai Mu**[1], **Dwijit GuhaSarkar**[3], **Anat O. Stemmer-Rachamimov**[4], **Miguel Sena-Esteves**[3], **Christian E. Badr**[1,*], and **Casey A. Maguire**[1,*]

[1]Department of Neurology, The Massachusetts General Hospital, and NeuroDiscovery Center, Harvard Medical School, Boston, MA.

[2]Alzheimer Research Unit, The Massachusetts General Hospital Institute for Neurodegenerative Disease, Charlestown, MA.

[3]University of Massachusetts Medical School, Worcester, MA.

[4]Molecular Pathology Division, The Massachusetts General Hospital, Boston, MA.

[5]Department of Human Anatomy, Faculty of Medicine and Health Sciences, Universiti Putra Malaysia, Malaysia.

Abstract

The malignant primary brain tumor, glioblastoma (GBM) is generally incurable. New approaches are desperately needed. Adeno-associated virus (AAV) vector-mediated delivery of anti-tumor transgenes is a promising strategy, however direct injection leads to focal transgene spread in tumor and rapid tumor division dilutes out the extra-chromosomal AAV genome, limiting duration of transgene expression. Intravenous (IV) injection gives widespread distribution of AAV in normal brain, however poor transgene expression in tumor, and high expression in non-target cells which may lead to ineffective therapy and high toxicity, respectively. Delivery of transgenes encoding secreted, anti-tumor proteins to tumor stromal cells may provide a more stable and localized reservoir of therapy as they are more differentiated than fast-dividing tumor cells. Reactive astrocytes and tumor-associated macrophage/microglia (TAMs) are stromal cells that comprise a large portion of the tumor mass and are associated with tumorigenesis. In mouse models of GBM, we used IV delivery of exosome-associated AAV vectors driving green fluorescent protein expression by specific promoters (NF-κB-responsive promoter and a truncated glial fibrillary acidic protein promoter), to obtain targeted transduction of TAMs and reactive astrocytes, respectively, while avoiding transgene expression in the periphery. We used our

*Corresponding authors: Casey A. Maguire, cmaguire@mgh.harvard.edu, Telephone: (617) 726-5725, Fax: (617) 724-1537, Christian E. Badr, badr.christian@mgh.harvard.edu, Telephone: (617)-643-3485, Fax: (617) 724-1537.

Author contributions.

CAM and CB conceived of the study. AV, CAM, SGL, JSN, DJP, PSC, AM, ZF, EH, KP, SG, DM, DG, CB performed experiments. CAM, CB, SGL, AV, MSE, DG, ASR, BTH analyzed the results. CAM and CB wrote the manuscript with input from all authors. All the authors read and approved the final version of the manuscript.

Conflict of interest CAM has submitted patent applications regarding the exo-AAV platform. CAM holds equity in and is a founder and scientific advisor of Chameleon Biosciences, Inc, a gene therapy company.

approach to express the potent, yet toxic anti-tumor cytokine, interferon beta, in tumor stroma of a mouse model of GBM, and achieved a modest, yet significant enhancement in survival compared to controls. Noninvasive genetic modification of tumor microenvironment represents a promising approach for therapy against cancers. Additionally, the vectors described here may facilitate basic research in the study of tumor stromal cells *in situ*.

INTRODUCTION

Standard-of-care treatment for GBM involves radiation, chemotherapy, and maximal surgical resection of the tumor. As the 5 year survival rate of 4.7% indicates[1], these treatments have not been effective in preventing disease progression. Oncolytic viruses have shown promise for treating GBM, however the host's anti-viral immune response can reduce virus spread throughout tumor[2]. Adeno-associated virus (AAV) vector delivery of anti-tumor genes to remaining malignant cells after resection has potential to prevent recurrence. Unfortunately, current AAV vectors have been rather slow to progress further than preclinical mouse models of GBM. One likely reason is minimal spread of vector after direct intratumoral injection[3–5]. The second is the extrachromosomal nature of AAV vectors leads to rapid dilution in dividing tumor cells and loss of therapeutic transgene expression[6]. Our group[7–9] and subsequently others[10] have proposed genetically modifying normal brain with secreted anti-tumor proteins. While this does show substantial efficacy in mouse models of GBM, a possible drawback is the requirement to genetically modify large numbers of healthy cells which has potential safety issues and requires efficient secretion of anti-tumor protein. As brain and brain tumors are highly vascularized, delivery of therapies via the blood stream is an attractive approach for widespread transgene delivery. Some AAV vector serotypes cross the blood-brain barrier (BBB) and mediate widespread gene transfer to neurons, astrocytes and endothelial cells[11, 12]. However, current AAV vector systems are suboptimal for intravascular (i.v.) gene delivery to the brain due to pre-existing immunity to the virus (e.g. neutralizing antibodies to the virus capsid)[13]. Also, suboptimal tissue/transcriptional targeting results in low levels of transgene expression in tumor cells[3] and high expression in liver with potential toxic side-effects. A promising target for therapy is tumor stromal cells (Fig. 1). Many tumor types, including GBM have high amounts of stromal cells such as tumor-associated myeloid-derived cells (TAMs, which include monocytes, macrophage, microglia)[14], reactive astrocytes[15], and cancer associated fibroblasts[16]. In general, systemically injected AAV does not transduce microglia and macrophage *in vivo* in mice[11], although some limited success has been reported with direct intracranial injection[17, 18].

Recently we have described a hybrid gene delivery system comprised of AAV associated with exosomes called exo-AAV[19]. We have demonstrated that exo-AAV has certain advantages for *in vivo* gene delivery in preclinical models, including evasion of anti-AAV antibodies[20] and better gene delivery to CNS at low vector doses[21]. Using exo-AAV for gene delivery via the systemic route, we tested whether tumor-microenvironment inducible promoters would result in gene delivery to brain tumor stroma.

MATERIALS AND METHODS:

Cells:

Human 293T cells were obtained from the American Type Culture Collection (Manassas, VA) and cultured in high glucose Dulbecco's modified Eagle's medium (DMEM, Life Technologies, Grand Island, NY) supplemented with 10% fetal bovine serum (Sigma, St Louis, MO), 100 U/ml penicillin, and 100 μg/ml streptomycin (Life Technologies) in a humidified atmosphere supplemented with 5% CO2 at 37°C. Murine GL261 cells (National Cancer Institute) were cultured in RPMI 1640 media (Life Technologies, Grand Island, NY) supplemented with 10% fetal bovine serum (Sigma, St Louis, MO), 100 U/ml penicillin, and 100 μg/ml streptomycin and cultured under the same conditions as for 293T cells. Primary human GSCs used in this study were obtained from the Ohio State University James Comprehensive Cancer Center[22]. GSCs were cultured as neurospheres in Neurobasal medium (Gibco) supplemented with Heparin, B27, recombinant human endothelial growth factor (EGF) and basic fibroblast growth factor (bFGF).

AAV plasmids:

For immunofluorescence analysis of transduced cell types we used a self-complementary (sc) AAV construct encoding GFP driven by the hybrid CMV-enhancer/chicken beta actin (CBA) promoter (sc-AAV-CBA-GFP) or the same construct with the promoter replaced with the 5NF promoter[23, 24] called sc-AAV-5NF-GFP. To construct an AAV vector encoding murine interferon beta (mIFN-β) under the 5NF promoter, murine codon-optimized mIFN-β was synthesized and cloned into pUC57 plasmid by Genscript (Piscataway, NJ). Next the GFP transgene was removed from scAAV-5NF-GFP and the backbone ligated with the similarly digested mIFN-β cDNA place to create scAAV-5NF-mIFN-β. To generate scAAV-GFAP-mIFN-b, a scAAV plasmid encoding ApoE2 under the truncated GFAP promoter, gfa2ABC$_1$D[25] (AAV-GFAP-ApoE2) had the ApoE2 insert removed with a NcoI and BamHI digest. Next we PCR amplified codon-optimized mIFN-β using Phusion polymerase (NEB) and flanking primers, forward (AGTCCTTCATGAGCCACCATGAACAATCGGTGGATCC), reverse (TGTCATAGATCTTTAATTCTGGAAGTTTCTGGTC). As the mIFN-β cDNA had internal NcoI and BamHI sites we designed the primers to contain different restriction sites which generate compatible ends for these sites. The forward primer contains a BspHI site compatible with the upstream NcoI site and the reverse primer a BglII site which is compatible with the downstream BamHI site in the AAV plasmid. The mIFN-β PCR product was digested with NcoI and BglII and ligated with NcoI/BamHI digested AAV-GFAP to generate AAV-GFAP-mIFN-β. To generate scAAV-GFAP-null (devoid of transgene), digesting out the ApoE2 fragment using flanking upstream and downstream XbaI sites and then ligating the XbaI sites together.

exo-AAV preparations:

exo-AAV were produced in 293T cells as previously described[26]. Briefly, a triple transfection of AAV plasmid, rep/cap plasmid (AAV9 serotype used) and helper plasmids was performed using the calcium phosphate method in ten 15 cm dishes. Media was changed to 2% FBS in DMEM the day after transfection and to exosomes-free 2% FBS at

48h post transfection. At 72 h post transfection, media was harvested. Cell debris and apoptotic bodies were removed by sequential, 10 min 300 × g and 2000 × g centrifugations, respectively. The supernatant containing exo-AAV was then centrifuged at 20,000 × g for 1 h to deplete larger microvesicles. Next, the remaining media was centrifuged at 100,000 × g for 1 hour using a Type 70 Ti rotor in an Optima™ L-90K ultracentrifuge (both Beckman Coulter, Inc., Indianapolis IN). The resulting pelleted material was resuspended in serum-free, antibiotic-free DMEM. exo-AAV preparations were stored at −80°C until use. Before titration, exo-AAV sample was treated with DNase to remove plasmid DNA from the transfection by mixing 5 μl of the sample with 1 μl DNase I, 5 μl 10× buffer, and 39 μl water. Samples were incubated 1 h at 37°C and then Dnase I was inactivated at 75°C for 15 min. To ensure accurate titration of exo-AAV which contains protein and lipids, we purified AAV genomes using High Pure Viral Nucleic Acid Kit (Roche, Indianapolis, IN). This kit contains detergents and proteinase K to degrade and lyse membraned viruses and is also certified to remove PCR inhibitors. Next, exo-AAV preparations were titered using a quantitative TaqMan PCR that detects AAV genomes (polyA region of the transgene cassette) was performed as previously described[27].

Animals and injections:

All animal experiments were approved by the Massachusetts General Hospital Subcommittee on Research Animal Care following guidelines set forth by the National Institutes of Health Guide for the Care and Use of Laboratory Animals. Female athymic nude mice aged 6–8 weeks were purchased from Charles River Laboratories (Wilmington, MA). Female C57BL/6 mice aged 6–8 weeks were purchased from Jackson Laboratory (Bar Harbor, ME). For tail vein injections of exo-AAV, mice were placed into a restrainer, (Braintree Scientific, Inc., Braintree, MA). Next the tail was warmed in 40°C water for 30 seconds, before wiping the tail with 70% isopropyl alcohol pads. A 100–300 μl volume of vector (dose indicated in results section) was slowly injected into a lateral tail vein, before gently finger clamping the injection site until bleeding stopped. For implantation of tumor cells, mice were anesthetized with a mixture of 100 mg/kg ketamine and 5 mg/kg xylazine in 0.9% sterile saline. Mice were placed in a stereotaxic frame and intracranially injected into the striatum with 2×10^4 murine GL261-FLuc cells (female C57BL/6 mice) or 2×10^4 human GSCs (female nude mice) using a Micro 4 Microsyringe Pump Controller (World Precision Instruments, Sarasota, FL) attached to a Hamilton syringe with a 30-gauge needle (Hamilton, Reno, NV), at the following coordinates in mm from bregma: +0.5 antero-posterior, +2.0 medio-lateral, −2.5 dorso-ventral.

Fluorescence, histology and immunohistochemistry:

Mice were anesthetized with an overdose of ketamine/xyalzine and transcardially perfused with PBS for 3 minutes to flush out blood, followed by 4% formaldehyde in PBS for 7 minutes to fix tissues. The brain and liver from each mouse were collected, post-fixed for 48 hours in 4% formaldehyde in PBS at 4°C and then transferred to 30% sucrose in PBS for 48 – 72 hours at 4°C for cryoprotection. Tissues were embedded in Neg-50 frozen section medium (Fisher Scientific) using a dry ice/2-methyl-butane bath and mounted in a Microm HM550 cryostat (Thermo Scientific). Throughout the brain/brain tumor or liver, 40 μm-thick coronal sections were collected and transferred to a 12-well plate containing PBS kept on ice

and stored at 4°C. Immunofluorescence was performed on these free-floating sections. The sections were permeabilized for 2h using 0.5% Triton X-100 in PBS and non-specific binding was blocked with 5% normal goat serum (NGS) in PBS.

For staining of tumor associated myeloid derived cells: primary antibody specific for GFP (1:400 dilution, rabbit anti-GFP, ABfinity, Life Technologies) was diluted in 1.5% NGS in PBS and incubated for 60 hours at 4°C in stirring condition. Next, 1:1000 diluted secondary antibody (goat anti-rabbit Alexa Fluor 488, Cell Signaling) was incubated for 1 hour at room temperature in stirring condition. Sections were co-stained with rat anti-mouse CD68 IgG monoclonal antibody (Clone FA-11, Bio-Rad, Raleigh, NC). Next secondary Alexa594-conjugated goat anti-rat IgG was added at 1:1000 dilution. Nucleic staining was performed with DAPI, and, after final washes in PBS, sections were carefully mounted onto slides using a brush and dried overnight. Finally, Fluorescence Mounting Medium (Dako North America, Carpinteria, CA) was applied and sections were covered with a coverslip. Tile-scan images were collected on a Zeiss Axio Imager Z epifluorescence microscope equipped with AxioVision software and modified for automated acquisition of entire brain slices, using either 5×, 10× or 20× objectives. In some experiments, images were acquired on a Nikon Eclipse TE2000 inverted fluorescence microscope (Nikon, Melville, NY) fitted with a Zyla 5.5 megapixel monochrome sCMOS camera (Andor, Belfast, UK) connected to Nikon Elements software (Nikon).

For colocalization of exo-AAV expressed GFP with either CD68 stained cells or tumors expressing mCherry, slides were analyzed with confocal imaging using a Zeiss LSM 5 Pascal laser-scanning confocal microscope (Zeiss, Oberkochen, Germany). Images were acquired using a 10, 40 or 63 PlanApo (NA 1.4) differential interference contrast (DIC) objective on an inverted microscope (Axiovert 200 M, Zeiss) equipped with an LSM 510META scan head (Zeiss). Argon ion (488 nm) and HeNe (543 nm) lasers were used for excitation. Green and red fluorescence emissions were detected through BP 505–530 and 560–615 filters, respectively.

Quantitation of transduced CD68+ cells within tumor sections.

The percentage of $CD68^+$ cells within tumors was estimated by ImageJ analysis software[28] analysis of high magnification images of tissue sections ($CD68^+$ cells stained red, and GFP positive cells stained green as described above. First, a threshold range was set across all the images to identify CD68+ cells as ROI's (regions of interest). Next, the identified ROI's from each image was summarized in a ROI manager to determine the area, count and mean values. Next, we manually counted GFP positive cells in images that colocalized with CD68 signal. The percentage of CD68+ cells which expressed GFP was calculated using the following equation: (# of GFP^+, $CD68^+$ cells)/(total number of $CD68^+$) cells x100.

For staining of reactive astrocytes:

Primary chicken anti-GFP antibody (1:500 dilution, GFP-1020; Aves Labs, Tigard, OR) was co-incubated with primary rabbit anti-GFAP antibody (1:500 dilution, G969, Sigma) for 48 h followed by detection with 1:500 dilutions of Alexa-488-goat anti-chicken (for GFP) and Cy3-goat anti-rabbit (for GFAP).

Hematoxylin and eosin (H&E) staining and pathological analysis:

20 μm sections from fresh-frozen brains were made in a Model cryostat (Company, City State). H&E staining was performed according to standard protocol.

Statistics:

Statistical analysis was performed using GraphPad Prism (v6.01; LaJolla, CA). A p-value ≤ 0.05 was considered statistically significant. For analysis between multiple groups, a one-way analysis of variance (ANOVA) was performed followed by a Sidak Multiple Comparison Test to compare individual groups. For survival analysis of Kaplan-Meier curves, we performed both a Log-rank (Mantel-Cox) test and a Gehan-Breslow-Wilcoxon test.

RESULTS

NF-κB inducible promoter mediates widespread reporter gene expression in tumor-associated myeloid-derived cells after systemic injection of exo-AAV in brain tumor-bearing mice.

We compared systemic administration of exo-AAV encoding either a broadly active promoter, chicken beta actin (CBA), or an NF-κB inducible promoter, 5NF[23, 24]. The latter promoter contains 5 tandem repeats of NF-κB binding sites followed by a TATA box. Nude mice were implanted with human glioma cancer stem-like cells (GSCs) and 10 days later mice were injected via the tail vein with 6×10^{11} genome copies (g.c.) of exo-AAV9-CBA-GFP or exo-AAV9–5NF-GFP (both n=4). Seven days later, mice were sacrificed and tissue cryosections analyzed by immunofluorescence for GFP expression. As expected the vector with the CBA promoter (broadly active promoter) gave widespread transduction of the brain (Fig 2A) as we have previously reported[21], sparse tumor transduction (Supplementary Fig.S1), and widespread liver transduction (Fig. 2C). In contrast exo-AAV9–5NF-GFP gave no detectable GFP in normal brain or liver (Fig. 2B, D). However, diffuse yet widespread transduction throughout the tumor was observed in analyzed sections (Fig. 3A, B). GFP positive cells did not co-localize with tumor-expressed mCherry using confocal microscopy (Fig. 3A, B). Instead, the GFP+ cells had distinct myeloid-derived cell-like morphology, which was confirmed by CD68 staining (in GSC tumors not-expressing mCherry) and GFP-colocalization by confocal imaging (Fig. 3C). Transduction of $CD68^+$ myeloid-derived cells was widespread throughout all tumor sections examined and ImageJ analysis revealed 13.25 +/− 6.68% of $CD68^+$ cells within serial sections of tumor were GFP positive. Transduced $CD68^+$ were located in all areas of tumor sections (from center to margin) with no apparent bias of distribution. We also tested conventional AAV9 packaging the 5NF-GFP expression cassette to transduce a mouse macrophage cell line, RAW cells, in the presence or absence of the NF-κB activating cytokine, TNF-α. AAV9 transduced RAW cells showed detectable GFP expression three days after vector addition TNF-α treatment resulted in a 20% increase in GFP signal, although this was not statistically significant (p=0.165, Supplementary Fig. S2).

A truncated GFAP promoter allows reporter gene expression in reactive astrocytes after systemic injection of exo-AAV9 in brain tumor bearing mice.

Reactive astrocytes have been reported at the tumor periphery in postmortem human GBM samples[29] as well as implicated in tumor aggressiveness in preclinical GBM models[15, 30]. As glial fibrillary acidic protein, GFAP, is strongly expressed in reactive astrocytes, we engineered an exo-AAV vector with a truncated GFAP promoter, gfa2ABC$_1$D[25] (called GFAP) driving GFP expression. Recently we have shown that systemically injected AAV9-GFAP-GFP enables widespread transduction of astrocytes in naïve (no tumor) murine brain with no detectable reporter expression in liver[31]. We intracranially implanted C57BL/6 mice with murine GL261 glioma cells (we used these cells as they have been shown to be responsive to reactive astrocytes[15]). Fourteen days post-tumor implantation, mice were i.v. injected with exo-AAV9-GFAP-GFP (n=3, 2×10^{12} g.c.) and at 24 days post-tumor (10 days post-vector), mice were sacrificed, and brains and organs processed for immunofluorescence analysis. Tumor sections were immunostained for both GFP and GFAP. Robust GFP expression was observed in GFAP-positive astrocytes at the tumor border; in addition, intensely green fluorescent cells extended into the tumor (Fig. 4, Supplementary Fig. S3). These cells did not show clear GFAP staining, although we have reported that this promoter construct in active in both GFAP positive and negative astrocytes[31]. There is a possibility, however, that these cells were tumor cells. Importantly, we also injected a subset of mice bearing GL261 brain tumors (n=3) i.v. with exo-AAV9–5NF-GFP and observed TAM transduction (Supplementary Fig.S4) as with the human GSC xenograft model in nude mice.

Transcriptionally-targeted transduction of brain tumor stromal cells with exo-AAV encoding murine IFN-β results in anti-glioma responses

To test whether genetic modification of GBM stromal cells with a model anti-tumor protein could exert control over growth of aggressive syngeneic GL261 tumors, we replaced the GFP cassette in both AAV-5NF-GFP and AAV-GFAP-GFP with cDNA encoding the murine interferon beta (mIFN-β). IFN-β is a cytokine with potent anti-tumor effects, although it can mediate systemic toxicity and animal death when delivered IV by AAV9 and expressed from strong ubiquitous promoters (Supplementary Fig. S5). To test the functionality of exo-AAV9–5NF-mIFN-β, we transduced RAW 264.7 murine macrophage cells with this vector (10^7 gc/cell), or with exo-AAV9–5NF-GFP as control. Media was harvested three days post transduction and an IFN-b ELISA performed. We readily detected IFN-b in media from cells transduced with exo-AAV9–5NF-mIFN-β (2,273 +/− 106 pg/ml) but not the control vector (Supplementary Fig. S6). To test the ability of exo-AAV9–5NF- mIFN-β to treat aggressive GBM tumors, we tried two different treatment strategies. The first was a “late therapy” model in which we implanted mice intracranially with 5×10^4 GL261 cells followed by i.v. injection of either exo-AAV-5NF-GFP as control or exo-AAV-5NF-mIFN-β on day 12 post tumor (7.5×10^{11} g.c injected). In the “early treatment” model mice were injected with 2×10^4 GL261 cells followed by i.v. injection of either vector day 7 post tumor (4.7×10^{11} g.c injected). In both experiments, each group was comprised on n=8 mice. We monitored mouse survival via a predetermined humane endpoint, including body weight loss (>20%), hemiparesis, and hunching. In both the late (Fig. 5A) and early (Fig. 5B) treatment models we observed a very modest ~2 day (5–9%) increase in median survival which was not statistically significant.

Histopathological analysis of the brains revealed approximately 10–20% cell death (seen as foci of necrosis) in mIFN-β-treated brains compared to minimal death in the control group in which cell death was mostly limited to scattered apoptotic cells. Necrosis was more prominent in the early treatment model (5B).

Next, we tested whether expression of mIFN-β in reactive astrocytes around the GL261 tumor could enhance animal survival. First we tested for functional expression of vector-encoded mIFN-β after systemically delivered exo-AAV9-GFAP-mIFN-β. Non-tumor bearing C57BL/6 mice (n=3) were injected i.v. with either vehicle (PBS) or 4×10^{11} g.c. of exo-AAV9-GFAP-mIFN-β and two weeks later sacrificed and RNA harvested from brain for RT-qPCR analysis of mIFN-β mRNA levels. We found that mice weight remained stable over the time period examined, suggesting no overt toxicity at this dose. Furthermore, mIFN-β transcript was detected in all mice injected with exo-AAV9-GFAP-mIFN-β, but not vehicle control (Supplementary Fig. S7A). By ELISA, we also detected mIFN-β in media of primary mouse astrocytes transduced by exo-AAV9-GFAP-mIFN-β (1,753 +/− 258 pg/ml) but not when transduced by the control vector (Supplementary Fig. S7B).

Next, mice (n=6 per group) were injected intracranially with 2×10^{4} GL261 cells and one week later, injected with 3×10^{11} g.c. of exo-AAV9-GFAP-mIFN-β or the same dose of exo-AAV9-GFAP vector devoid of transgene (called exo-AAV9-GFAP-null). We also tested exo-AAV9-GFAP-mIFN-β at a lower dose of 8×10^{10} g.c. We observed a 14% increase in median survival with the higher dose of exo-AAV9-GFAP-mIFN-β over exo-AAV9-GFAP-null (Fig. 6, p=0.02, Log-rank test). The lower dose of exo-AAV9-GFAP-mIFN-β had virtually identical median survival as the control group (Fig. 6).

Histopathological analysis of control and treated brains revealed large areas of necrosis comprising 40%−50% of the tumor in mIFN-β treated mice compared to scattered apoptotic cells in the control group (Fig. 6). We observed that the area of necrosis appeared to be at the tumor core. As we had shown with the exo-AAV9-GFAP-GFP vector transgene expression to be localized mainly to reactive astrocytes at the tumor border (Fig 4), we extracted tissue samples from three different areas: the tumor core, just outside the tumor core, and in the normal brain surrounding the tumor. We also isolated normal brain from exo-AAV9-GFAP-null mice as control. Next RT-qPCR was performed to detect m-IFN-β and we normalized the Ct values to GAPDH. As expected, the highest mIFN-β mRNA was found in the brain surrounding the tumor, supporting our data with the GFP reporter (Supplementary Fig. S7C).

DISCUSSION:

In this study, we demonstrate that targeted transduction of brain tumor stromal cells can be achieved after systemic injection of an AAV-based vector system using promoters responsive to the tumor microenvironment. We utilized exo-AAV in this study has we have previously shown that this vector system has attributes such as enhanced transduction to CNS[21], liver[32], inner ear[33], and retina[34] compared to conventional AAV. Exo-AAV also has a benefit of antibody evasion which may have clinical relevance in patients with pre-existing humoral immunity to AAV[20, 32]. That said, it is likely conventional AAV vectors will also transduce

tumor stroma. First, we have shown that exo-AAV and AAV to have similar target (astrocytes, neurons) when transgene expression is driven by a broadly active promoter (CBA)[21]. Second, we have recently demonstrated that we can achieve widespread astrocyte transduction with systemically injected conventional AAV9 with transgene driven by the GFAP promoter[31]. Finally, in cultured RAW cells (macrophage) we found that conventional AAV9 with the 5NF-GFP cassette could drive robust GFP expression (Supplementary Fig S2). Future work will confirm whether we achieve enhancement in TAM or reactive astrocyte transduction with exo-AAV vs. conventional AAV.

There is limited data demonstrating transduction of myeloid-derived cells with AAV vectors. The existing data showing modest macrophage/microglia transduction in the CNS was performed after direct AAV injection[17, 18]. On the other hand, we achieved selective transduction of myeloid-derived cells after systemic injection of exo-AAV9 using a NF-κB regulated promoter. Successful transduction of this cell type may require several important factors including: (a) the ability of the vector to traffic to and enter the cell, and (b) appropriate promoter responsive to the *in vivo* environmental conditions. We observed that under identical vector/microenvironment conditions with exo-AAV9, switching the promoter from CBA to 5NF changed the transduction profile from primarily neurons and astrocytes in the CNS and hepatocytes in the liver to myeloid-derived, tumor-associated cells with undetectable hepatocyte transduction. It is becoming evident that broadly active promoters such as CMV and CBA may not be highly active in all subsets of cells. For example, we observed that systemic injection of an AAV9 vector encoding GFP under the synapsin promoter increased the percentage of GFP-positive neurons by 7-fold compared to the same AAV9 vector driving GFP with a CBA promoter[31]. Another important consideration is the translation potential of these findings to humans. While AAV transduction of microglia and macrophage is very limited in mice, one report found that in non-human primates (NHPs), the cells primarily transduced by systemically injected AAV9 (using a CBA promoter) were microglia (Iba-1+) and astrocytes (GFAP+)[35]. This is promising for the potential translation of our stromal cell targeting strategy, although further research in NHPs needs to be performed to confirm these findings. The transcription factor NF-κB is often active in tumors and tumor-associated macrophage/microglia compared to other cells[36–38]. While we cannot rule out expression of mIFN-β from transduced tumor cells in the GL261 model, the majority of the response likely came from TAMS, as we did not detect GFP expression in tumor cells *in vivo* with the AAV-5NF-GFP construct and the high division of tumor cells dilutes out the AAV genome. Similarly, gliomas can express varying amounts of GFAP, however we did not observe widespread GFP immunostaining of GL261 tumor sections in mice injected with exo-AAV9-GFAP-GFP and high grade glioma often lose GFAP expression[39], indicating reactive astrocytes at the tumor border as a driver of therapeutic mIFN-β in this model. This is also supported by the increased mRNA expression of mIFN-β at the periphery of the tumor as compared to the tumor core in the brain of mice injected with exo-AAV9-GFAP- mIFN-β. (Supplementary Fig. S7C). The reason for increased necrosis in the tumor core is not clear at present. One possible explanation is that, due to differences in the tumor microenvironment, cells at the tumor core might be more susceptible to this secreted cytokine. We observed a modest yet significant (14%) increase in survival using the astrocyte-based mIFN-β expression at 3×10^{11} gc/mouse. While

encouraging, there are potential limitation of using IFN-β as an anti-tumor protein. While we mitigated the potent toxicity observed with lower doses of systemically injected AAV9 driving mIFN-β expression with broadly active promoters (Fig. S5), increasing the dose of exo-AAV9-GFAP- mIFN-β two-fold (6×10^{11} gc/mouse), resulted in *reduced* survival of exo-AAV9-GFAP- mIFN-β-treated mice over the control group (data not shown). This likely indicates that at least in the experimental context described here, the therapeutic window of IFN-β is quite narrow. There is support in the literature for toxicity mediated by vector-encoded mIFN-β this observation[40], including some of our own work. Recently we reported survival results of intracranial injection of AAV encoding mIFN-β driven by different promoters in a GL261 brain tumor model[41]. While we found that with some promoter/mIFN-β combinations (likely ones with weaker activity) survival was increased over control treated groups, some of the promoters actually decreased animal survival, likely due to an inflammatory response[41].

Multiple studies, including our own, have evaluated the combination of IFN-β with Temozolomide (TMZ), the standard-of-care chemotherapeutic for GBM patients[42] (on mature GBM cells and Glioma stem cells both in culture and in vivo[41,43–47]). Such combination therapy was also evaluated on GBM patients[48, 49]. These studies have concluded that IFN-β increases sensitivity to TMZ and was well tolerated in phase I clinical studies[48, 49], and has been shown to enhance the therapeutic outcome[41]. Thus, it may be possible to use tumor stromal cells modified to produce IFN-β at sub-toxic doses and achieve tumor killing. Therefore, we anticipate that combining our exo-AAV9-IFN-β strategy (using GFAP or 5NF promoters) with TMZ could potently enhance the therapeutic response/survival and will be evaluated in future studies.

Alternatively, it may be prudent to test other secreted proteins (e.g. tumor necrosis factor-related apoptosis-inducing ligand, TRAIL) which have a larger therapeutic window and lower toxicity profile than IFN-β. This will allow us to use higher doses of vector to achieve transduction of more tumor stromal cells, increasing therapeutic efficacy. It may also be useful to simultaneous injection of both vectors (GFAP and NF-κB-regulated expression) to increase therapeutic efficacy, as this would treat the tumor from the outside (reactive astrocytes) and inside (myeloid-derived cells). We and others have shown ionizing radiation (IR) to activate the NF-κB signaling pathway in tumor cells[24, 36, 50, 51]. Radiation also activates NF-κB transcriptional activity in human myeloid cells by stimulating overall cytokine production such a TNF-α, a potent inducer of NF-κB[52, 53]. As radiation is standard care for GBM, it may serve to enhance induction of production of therapeutic protein in cells transduced by AAV-5NF vector.

Another application of this stromal cell transduction strategy is modulation of phenotype and effector function of these cell types for basic scientific study as well as creating a less-favorable environment for tumor cell proliferation. While the literature on TAMs role in tumorigenesis is rapidly expanding, there is less known regarding the role of astrogliosis in brain tumor progression. A hallmark of GBM in both postmortem human samples as well as mouse models is the prominent band of reactive astrocytes at the tumor margin without substantial penetration into the tumor core[29]. Furthermore, experimental models have demonstrated that astrocytes can increase invasiveness of GBM stem-like cells (GSCs)[54].

Using the exo-AAV-GFAP gene delivery system to modulate expression of mRNA/miRNAs in astrocytes may facilitate a better understanding of the astrocyte/tumor interaction.

CONCLUSION

We demonstrated that an AAV-based gene delivery system can transduce brain tumor stromal cells after non-invasive systemic injection and that we can obtain a therapeutic killing of tumor cells using these cells as a base for expression of secreted anti-tumor proteins. To our knowledge, on-site transduction of tumor- associated macrophage/microglia after systemic vector delivery has not been previously reported. This system could be applied to other tumor models with high tumor stromal cell content (e.g. breast cancers), tailoring transgene expression to the promoter activity of the specific stromal cell types.

Supplementary Material

Refer to Web version on PubMed Central for supplementary material.

ACKNOWLEDGMENTS

We thank the MGH Quantitative Real-Time PCR Core Facility for use of the quantitative PCR equipment for AAV quantitation and RT-qPCR analysis of transgene expression.

Funding. This work was supported by an American Brain Tumor Association Discovery Grant (CAM), a Cure Alzheimer's Fund award (CAM) and the National Institutes of Health, the National Cancer Institute K22CA197053 (C.E.B.).

REFERENCES

1. Dolecek TA, Propp JM, Stroup NE, and Kruchko C, CBTRUS statistical report: primary brain and central nervous system tumors diagnosed in the United States in 2005–2009. Neuro Oncol. 14 Suppl 5: p. v1–49.
2. Wakimoto H, Johnson PR, Knipe DM, and Chiocca EA, Effects of innate immunity on herpes simplex virus and its ability to kill tumor cells. Gene Ther, 2003 10(11): p. 983–90. [PubMed: 12756419]
3. Harding TC, Lalani AS, Roberts BN, Yendluri S, Luan B, Koprivnikar KE, Gonzalez-Edick M, Huan-Tu G, Musterer R, VanRoey MJ, Ozawa T, LeCouter RA, Deen D, Dickinson PJ, and Jooss K, AAV serotype 8-mediated gene delivery of a soluble VEGF receptor to the CNS for the treatment of glioblastoma. Mol Ther, 2006 13(5): p. 956–66. [PubMed: 16580881]
4. Wollmann G, Tattersall P, and van den Pol AN, Targeting human glioblastoma cells: comparison of nine viruses with oncolytic potential. J Virol, 2005 79(10): p. 6005–22. [PubMed: 15857987]
5. Harding TC, Dickinson PJ, Roberts BN, Yendluri S, Gonzalez-Edick M, Lecouteur RA, and Jooss KU, Enhanced gene transfer efficiency in the murine striatum and an orthotopic glioblastoma tumor model, using AAV-7- and AAV-8-pseudotyped vectors. Hum Gene Ther, 2006 17(8): p. 807–20. [PubMed: 16942441]
6. Hadaczek P, Mirek H, Berger MS, and Bankiewicz K, Limited efficacy of gene transfer in herpes simplex virus-thymidine kinase/ganciclovir gene therapy for brain tumors. J Neurosurg, 2005 102(2): p. 328–35. [PubMed: 15739562]
7. Maguire CA, Meijer DH, LeRoy SG, Tierney LA, Broekman ML, Costa FF, Breakefield XO, Stemmer-Rachamimov A, and Sena-Esteves M, Preventing growth of brain tumors by creating a zone of resistance. Mol Ther, 2008 16(10): p. 1695–702. [PubMed: 18714312]
8. Meijer DH, Maguire CA, LeRoy SG, and Sena-Esteves M, Controlling brain tumor growth by intraventricular administration of an AAV vector encoding IFN-beta. Cancer Gene Ther, 2009 16(8): p. 664–71. [PubMed: 19197327]

9. Crommentuijn MH, Maguire CA, Niers JM, Vandertop WP, Badr CE, Wurdinger T, and Tannous BA, Intracranial AAV-sTRAIL combined with lanatoside C prolongs survival in an orthotopic xenograft mouse model of invasive glioblastoma. Mol Oncol, 2015.
10. Hicks MJ, Funato K, Wang L, Aronowitz E, Dyke JP, Ballon DJ, Havlicek DF, Frenk EZ, De BP, Chiuchiolo MJ, Sondhi D, Hackett NR, Kaminsky SM, Tabar V, and Crystal RG, Genetic modification of neurons to express bevacizumab for local anti-angiogenesis treatment of glioblastoma. Cancer Gene Ther, 2015 22(1): p. 1–8. [PubMed: 25501993]
11. Foust KD, Nurre E, Montgomery CL, Hernandez A, Chan CM, and Kaspar BK, Intravascular AAV9 preferentially targets neonatal neurons and adult astrocytes. Nat Biotechnol, 2009 27(1): p. 59–65. [PubMed: 19098898]
12. Ahmed SS, Li H, Cao C, Sikoglu EM, Denninger AR, Su Q, Eaton S, Liso Navarro AA, Xie J, Szucs S, Zhang H, Moore C, Kirschner DA, Seyfried TN, Flotte TR, Matalon R, and Gao G, A single intravenous rAAV injection as late as P20 achieves efficacious and sustained CNS Gene therapy in Canavan mice. Mol Ther. 21(12): p. 2136–47.
13. Calcedo R, Vandenberghe LH, Gao G, Lin J, and Wilson JM, Worldwide epidemiology of neutralizing antibodies to adeno-associated viruses. J Infect Dis, 2009 199(3): p. 381–90. [PubMed: 19133809]
14. Glass R and Synowitz M, CNS macrophages and peripheral myeloid cells in brain tumours. Acta Neuropathol, 2014 128(3): p. 347–62. [PubMed: 24722970]
15. Okolie O, Bago JR, Schmid RS, Irvin DM, Bash RE, Miller CR, and Hingtgen SD, Reactive astrocytes potentiate tumor aggressiveness in a murine glioma resection and recurrence model. Neuro Oncol, 2016.
16. Clavreul A, Etcheverry A, Tetaud C, Rousseau A, Avril T, Henry C, Mosser J, and Menei P, Identification of two glioblastoma-associated stromal cell subtypes with different carcinogenic properties in histologically normal surgical margins. J Neurooncol, 2015 122(1): p. 1–10. [PubMed: 25503303]
17. Cucchiarini M, Ren XL, Perides G, and Terwilliger EF, Selective gene expression in brain microglia mediated via adeno-associated virus type 2 and type 5 vectors. Gene Ther, 2003 10(8): p. 657–67. [PubMed: 12692594]
18. Rosario AM, Cruz PE, Ceballos-Diaz C, Strickland MR, Siemienski Z, Pardo M, Schob KL, Li A, Aslanidi GV, Srivastava A, Golde TE, and Chakrabarty P, Microglia-specific targeting by novel capsid-modified AAV6 vectors. Mol Ther Methods Clin Dev, 2016 3: p. 16026. [PubMed: 27308302]
19. Gyorgy B and Maguire CA, Extracellular vesicles: nature's nanoparticles for improving gene transfer with adeno-associated virus vectors. Wiley Interdiscip Rev Nanomed Nanobiotechnol, 2017.
20. Gyorgy B, Fitzpatrick Z, Crommentuijn MH, Mu D, and Maguire CA, Naturally enveloped AAV vectors for shielding neutralizing antibodies and robust gene delivery in vivo. Biomaterials, 2014 35(26): p. 7598–609. [PubMed: 24917028]
21. Hudry E, Martin C, Gandhi S, Gyorgy B, Scheffer DI, Mu D, Merkel SF, Mingozzi F, Fitzpatrick Z, Dimant H, Masek M, Ragan T, Tan S, Brisson AR, Ramirez SH, Hyman BT, and Maguire CA, Exosome-associated AAV vector as a robust and convenient neuroscience tool. Gene Ther, 2016.
22. Mao P, Joshi K, Li J, Kim SH, Li P, Santana-Santos L, Luthra S, Chandran UR, Benos PV, Smith L, Wang M, Hu B, Cheng SY, Sobol RW, and Nakano I, Mesenchymal glioma stem cells are maintained by activated glycolytic metabolism involving aldehyde dehydrogenase 1A3. Proc Natl Acad Sci U S A, 2013 110(21): p. 8644–9. [PubMed: 23650391]
23. Badr CE, Niers JM, Morse D, Koelen JA, Vandertop P, Noske D, Wurdinger T, Zalloua PA, and Tannous BA, Suicidal gene therapy in an NF-kappaB-controlled tumor environment as monitored by a secreted blood reporter. Gene Ther, 2011 18(5): p. 445–51. [PubMed: 21150937]
24. Badr CE, Niers JM, Tjon-Kon-Fat LA, Noske DP, Wurdinger T, and Tannous BA, Real-time monitoring of nuclear factor kappaB activity in cultured cells and in animal models. Mol Imaging, 2009 8(5): p. 278–90. [PubMed: 19796605]
25. Lee Y, Messing A, Su M, and Brenner M, GFAP promoter elements required for region-specific and astrocyte-specific expression. Glia, 2008 56(5): p. 481–93. [PubMed: 18240313]

26. Maguire CA, Balaj L, Sivaraman S, Crommentuijn MH, Ericsson M, Mincheva-Nilsson L, Baranov V, Gianni D, Tannous BA, Sena-Esteves M, Breakefield XO, and Skog J, Microvesicle-associated AAV vector as a novel gene delivery system. Mol Ther, 2012 20(5): p. 960–71. [PubMed: 22314290]
27. Bennett J, Ashtari M, Wellman J, Marshall KA, Cyckowski LL, Chung DC, McCague S, Pierce EA, Chen Y, Bennicelli JL, Zhu X, Ying GS, Sun J, Wright JF, Auricchio A, Simonelli F, Shindler KS, Mingozzi F, High KA, and Maguire AM, AAV2 gene therapy readministration in three adults with congenital blindness. Sci Transl Med, 2012 4(120): p. 120ra15.
28. Schneider CA, Rasband WS, and Eliceiri KW, NIH Image to ImageJ: 25 years of image analysis. Nat Methods, 2012 9(7): p. 671–5. [PubMed: 22930834]
29. Nagashima G, Suzuki R, Asai J, and Fujimoto T, Immunohistochemical analysis of reactive astrocytes around glioblastoma: an immunohistochemical study of postmortem glioblastoma cases. Clin Neurol Neurosurg, 2002 104(2): p. 125–31. [PubMed: 11932042]
30. Lee J, Borboa AK, Baird A, and Eliceiri BP, Non-invasive quantification of brain tumor-induced astrogliosis. BMC Neurosci, 2011 12: p. 9. [PubMed: 21247490]
31. Dashkoff J, Lerner EP, Truong N, Klickstein JA, Fan Z, Mu D, Maguire CA, Hyman BT, and Hudry E, Tailored transgene expression to specific cell types in the central nervous system after peripheral injection with AAV9. Mol Ther Methods Clin Dev, 2016 3: p. 16081. [PubMed: 27933308]
32. Meliani A, B. F, Fitzpatrick Z, Marmier S, Leborgne C, Collaud F, Sola MS, Charles S, Ronzitti G, Vignaud A, van Wittenberghe L, Marolleau B, Jouen F, Tan S, Boyer O, Christophe O, Brisson AR, Maguire CA, Mingozzi F, Enhanced liver gene transfer and evasion of pre-existing humoral immunity with exosome-enveloped AAV vectors. Blood Advances, 2017.
33. Gyorgy B, Sage C, Indzhykulian AA, Scheffer DI, Brisson AR, Tan S, Wu X, Volak A, Mu D, Tamvakologos PI, Li Y, Fitzpatrick Z, Ericsson M, Breakefield XO, Corey DP, and Maguire CA, Rescue of Hearing by Gene Delivery to Inner-Ear Hair Cells Using Exosome-Associated AAV. Mol Ther, 2017 25(2): p. 379–391. [PubMed: 28082074]
34. Wassmer SJ, Carvalho LS, Gyorgy B, Vandenberghe LH, and Maguire CA, Exosome-associated AAV2 vector mediates robust gene delivery into the murine retina upon intravitreal injection. Sci Rep, 2017 7: p. 45329. [PubMed: 28361998]
35. Bevan AK, Duque S, Foust KD, Morales PR, Braun L, Schmelzer L, Chan CM, McCrate M, Chicoine LG, Coley BD, Porensky PN, Kolb SJ, Mendell JR, Burghes AH, and Kaspar BK, Systemic gene delivery in large species for targeting spinal cord, brain, and peripheral tissues for pediatric disorders. Mol Ther, 2011 19(11): p. 1971–80. [PubMed: 21811247]
36. Bhat KP, Balasubramaniyan V, Vaillant B, Ezhilarasan R, Hummelink K, Hollingsworth F, Wani K, Heathcock L, James JD, Goodman LD, Conroy S, Long L, Lelic N, Wang S, Gumin J, Raj D, Kodama Y, Raghunathan A, Olar A, Joshi K, et al., Mesenchymal differentiation mediated by NF-kappaB promotes radiation resistance in glioblastoma. Cancer Cell, 2013 24(3): p. 331–46. [PubMed: 23993863]
37. Biswas SK and Lewis CE, NF-kappaB as a central regulator of macrophage function in tumors. J Leukoc Biol, 2010 88(5): p. 877–84. [PubMed: 20573802]
38. Escarcega RO, Fuentes-Alexandro S, Garcia-Carrasco M, Gatica A, and Zamora A, The transcription factor nuclear factor-kappa B and cancer. Clin Oncol (R Coll Radiol), 2007 19(2): p. 154–61. [PubMed: 17355113]
39. Wilhelmsson U, Eliasson C, Bjerkvig R, and Pekny M, Loss of GFAP expression in high-grade astrocytomas does not contribute to tumor development or progression. Oncogene, 2003 22(22): p. 3407–11. [PubMed: 12776191]
40. Tada H, Maron DJ, Choi EA, Barsoum J, Lei H, Xie Q, Liu W, Ellis L, Moscioni AD, Tazelaar J, Fawell S, Qin X, Propert KJ, Davis A, Fraker DL, Wilson JM, and Spitz FR, Systemic IFN-beta gene therapy results in long-term survival in mice with established colorectal liver metastases. J Clin Invest, 2001 108(1): p. 83–95. [PubMed: 11435460]
41. GuhaSarkar D, Neiswender J, Su Q, Gao G, and Sena-Esteves M, Intracranial AAV-IFN-beta gene therapy eliminates invasive xenograft glioblastoma and improves survival in orthotopic syngeneic murine model. Mol Oncol, 2017 11(2): p. 180–193. [PubMed: 28098415]

42. Hottinger AF, Stupp R, and Homicsko K, Standards of care and novel approaches in the management of glioblastoma multiforme. Chin J Cancer, 2014 33(1): p. 32–9. [PubMed: 24384238]
43. Shen D, Guo CC, Wang J, Qiu ZK, Sai K, Yang QY, Chen YS, Chen FR, Wang J, Panasci L, and Chen ZP, Interferon-alpha/beta enhances temozolomide activity against MGMT-positive glioma stem-like cells. Oncol Rep, 2015 34(5): p. 2715–21. [PubMed: 26329778]
44. Happold C, Roth P, Silginer M, Florea AM, Lamszus K, Frei K, Deenen R, Reifenberger G, and Weller M, Interferon-beta induces loss of spherogenicity and overcomes therapy resistance of glioblastoma stem cells. Mol Cancer Ther, 2014 13(4): p. 948–61. [PubMed: 24526161]
45. Natsume A, Wakabayashi T, Ishii D, Maruta H, Fujii M, Shimato S, Ito M, and Yoshida J, A combination of IFN-beta and temozolomide in human glioma xenograft models: implication of p53-mediated MGMT downregulation. Cancer Chemother Pharmacol, 2008 61(4): p. 653–9. [PubMed: 17564708]
46. Natsume A, Ishii D, Wakabayashi T, Tsuno T, Hatano H, Mizuno M, and Yoshida J, IFN-beta down-regulates the expression of DNA repair gene MGMT and sensitizes resistant glioma cells to temozolomide. Cancer Res, 2005 65(17): p. 7573–9. [PubMed: 16140920]
47. Park JH, Ryu CH, Kim MJ, and Jeun SS, Combination Therapy for Gliomas Using Temozolomide and Interferon-Beta Secreting Human Bone Marrow Derived Mesenchymal Stem Cells. J Korean Neurosurg Soc, 2015 57(5): p. 323–8. [PubMed: 26113958]
48. Wakabayashi T, Kayama T, Nishikawa R, Takahashi H, Hashimoto N, Takahashi J, Aoki T, Sugiyama K, Ogura M, Natsume A, and Yoshida J, A multicenter phase I trial of combination therapy with interferon-beta and temozolomide for high-grade gliomas (INTEGRA study): the final report. J Neurooncol, 2011 104(2): p. 573–7. [PubMed: 21327711]
49. Motomura K, Natsume A, Kishida Y, Higashi H, Kondo Y, Nakasu Y, Abe T, Namba H, Wakai K, and Wakabayashi T, Benefits of interferon-beta and temozolomide combination therapy for newly diagnosed primary glioblastoma with the unmethylated MGMT promoter: A multicenter study. Cancer, 2011 117(8): p. 1721–30. [PubMed: 21472719]
50. Brach MA, Hass R, Sherman ML, Gunji H, Weichselbaum R, and Kufe D, Ionizing radiation induces expression and binding activity of the nuclear factor kappa B. J Clin Invest, 1991 88(2): p. 691–5. [PubMed: 1864978]
51. Veuger SJ, Hunter JE, and Durkacz BW, Ionizing radiation-induced NF-kappaB activation requires PARP-1 function to confer radioresistance. Oncogene, 2009 28(6): p. 832–42. [PubMed: 19060926]
52. Sherman ML, Datta R, Hallahan DE, Weichselbaum RR, and Kufe DW, Regulation of tumor necrosis factor gene expression by ionizing radiation in human myeloid leukemia cells and peripheral blood monocytes. J Clin Invest, 1991 87(5): p. 1794–7. [PubMed: 2022746]
53. Iwamoto KS and McBride WH, Production of 13-hydroxyoctadecadienoic acid and tumor necrosis factor-alpha by murine peritoneal macrophages in response to irradiation. Radiat Res, 1994 139(1): p. 103–8. [PubMed: 8016298]
54. Rath BH, Fair JM, Jamal M, Camphausen K, and Tofilon PJ, Astrocytes enhance the invasion potential of glioblastoma stem-like cells. PLoS One, 2013 8(1): p. e54752. [PubMed: 23349962]
55. Liddelow SA, Guttenplan KA, Clarke LE, Bennett FC, Bohlen CJ, Schirmer L, Bennett ML, Munch AE, Chung WS, Peterson TC, Wilton DK, Frouin A, Napier BA, Panicker N, Kumar M, Buckwalter MS, Rowitch DH, Dawson VL, Dawson TM, Stevens B, et al., Neurotoxic reactive astrocytes are induced by activated microglia. Nature, 2017 541(7638): p. 481–487. [PubMed: 28099414]

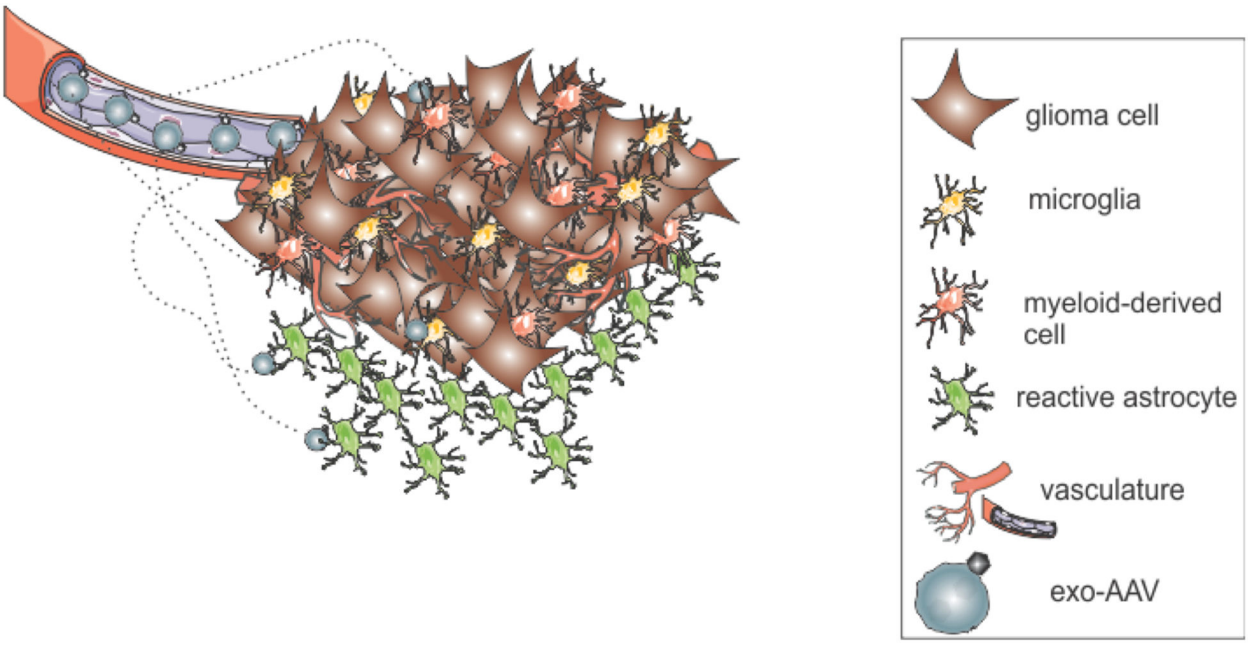

Figure 1. Stromal cell targeting strategy.

GBM's are comprised of many types of stromal cells, including tumor-associated myeloid-derived cells like macrophage and microglia, and reactive astrocytes. These cells represent a more attractive target for AAV-based therapies. Therapeutic genes are delivered to these cells using exosome-associated AAV (exo-AAV).

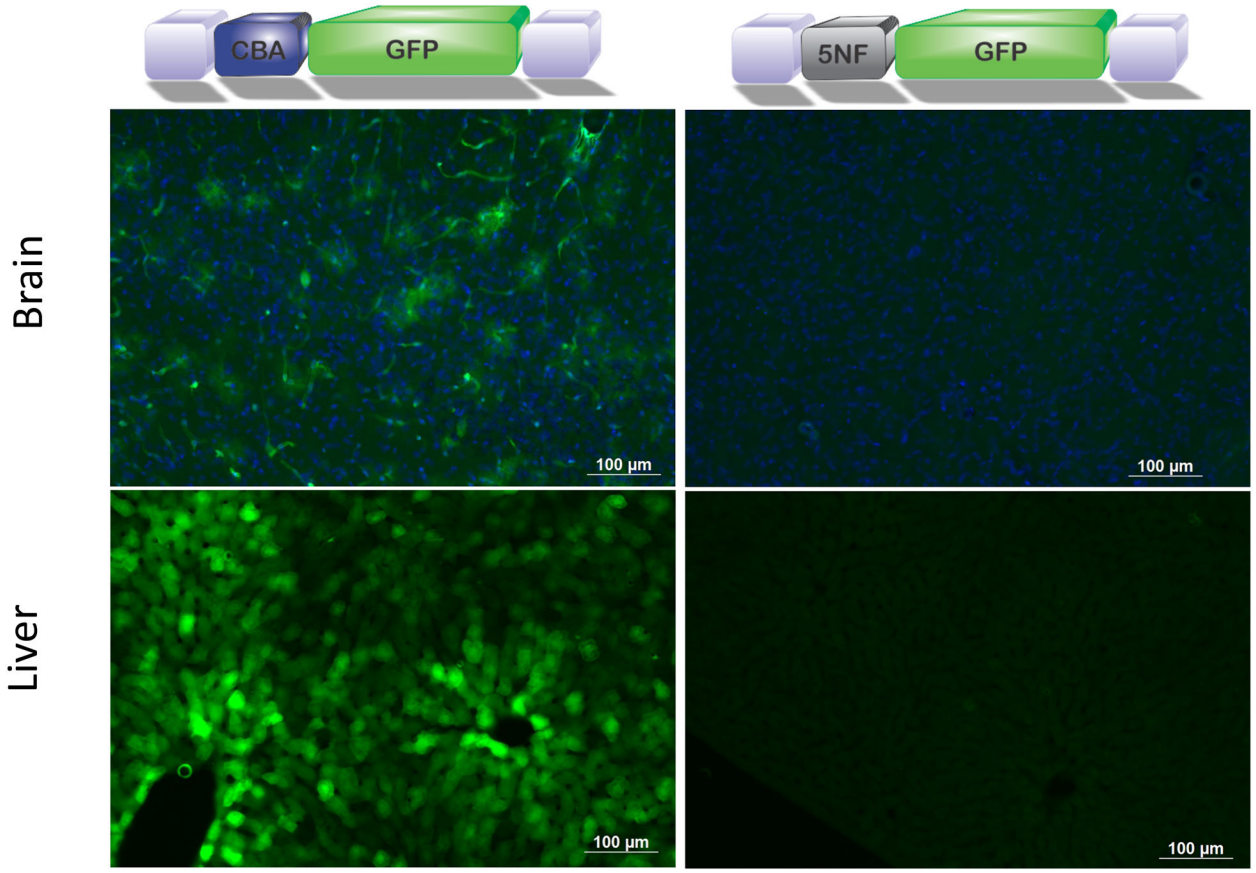

Figure 2. Systemic injection of exo-AAV9–5NF-GFP reduces off target expression of transgene in liver and normal brain.

Exo-AAV9-CBA-GFP mediates strong GFP expression in periphery and normal brain **(A, C)** after i.v. injection of mice bearing GBM tumors, while exo-AAV9–5NF-GFP does not detectably transduce liver or normal brain (**B, D**). Equal doses of each vector were injected.

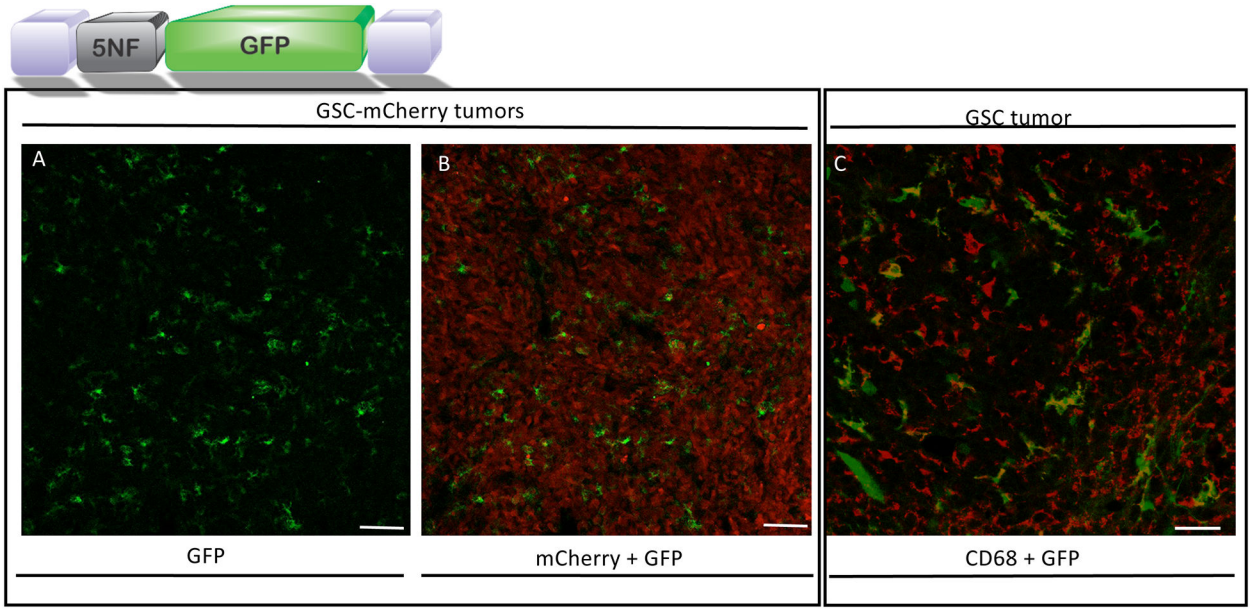

Figure 3. Systemic injection of exo-AAV9–5NF-GFP transduces tumor-associated myeloid derived cells in human glioma stem-like cell tumors in mice.

exo-AAV9–5NF-GFP transduction of brain tumor stromal cells after intravenous injection. Nude mice bearing intrastriatal human GSC tumors were injected i.v. with exo-AAV9–5NF-GFP (vector schematic shown above; purple blocks, AAV inverted terminal repeats; 5NF, NF-κB inducible promoter). Mice were sacrificed at the humane endpoint, tumors sectioned, and immunostained for GFP. **(A)** GFP expression in tumor stromal cells. **(B)** Merge of GFP signal with tumor cell-expressed mCherry to show that the transduced cells are within the tumor mass. Scale bar=100 μm. **(C)** exo-AAV9–5NF-GFP primarily transduces CD68+ myeloid-derived cells within human GBM tumor (no mCherry expression in this tumor. Confocal imaging of human GSC tumor-bearing mice injected i.v. with exo-AAV9-NF-GFP. Tumor sections were stained with myeloid-derived cell marker CD68 (red) and co-localization with GFP was readily detected. Scale bar= 50 μm.

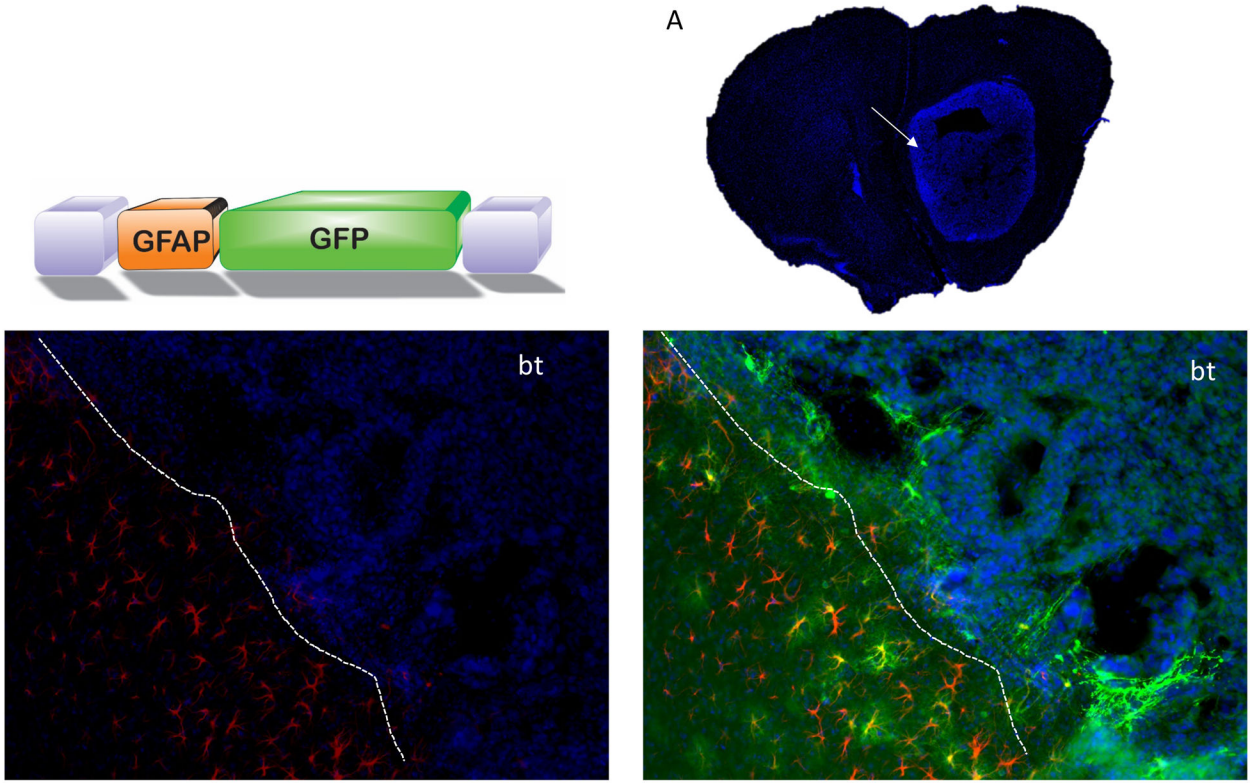

Figure 4. Exo-AAV9-GFAP-GFP transduces reactive astrocytes at brain/tumor interface in murine GL261 tumors after systemic injection.

AAV vector with truncated GFAP promoter driving GFP. **(A)** representative GL261 tumor section showing Dapi staining of tumor mass. **(B)** GFAP positive reactive astrocytes (red) at the tumor border indicated with dashed line. bt=brain tumor. **(C)** Widespread transduction of reactive astrocytes at tumor border. GFP positive astrocytes at tumor border are indicated with arrows. Representative GFP positive cells extending into the tumor (Dapi positive cells) are indicated by arrow heads.

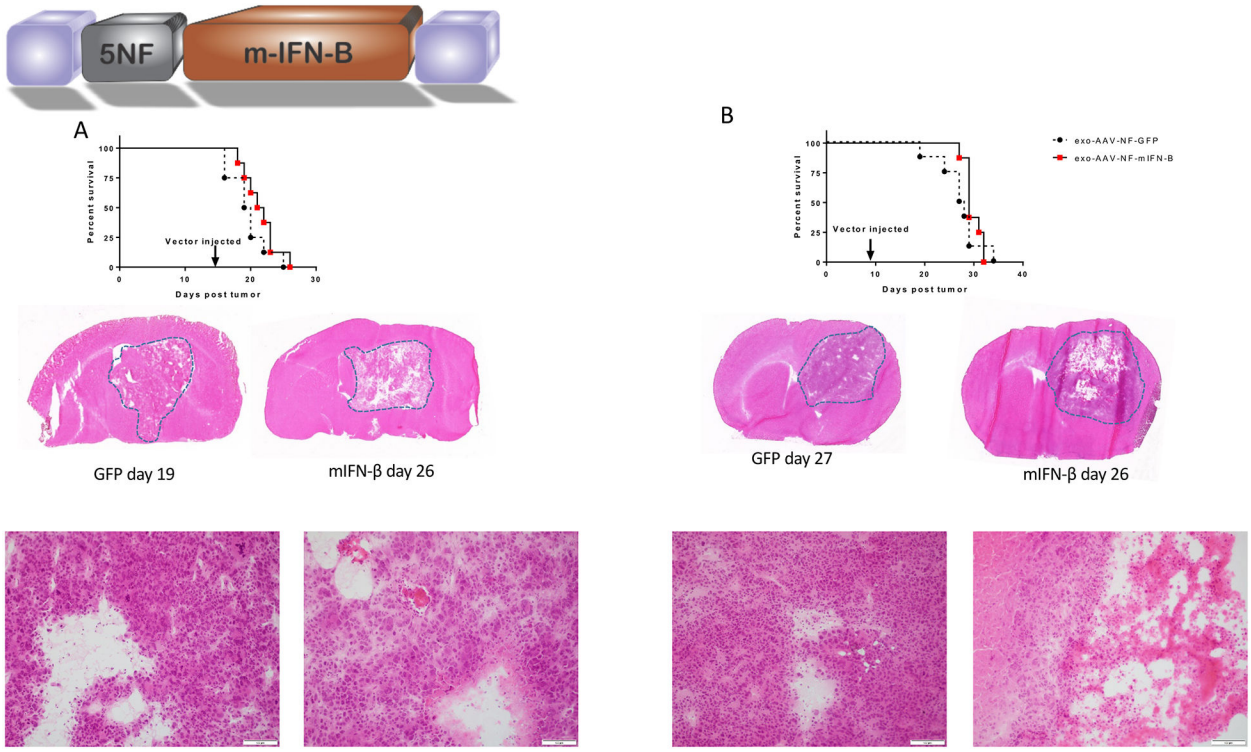

Figure 5. Systemically injected exo-AAV9–5NF-mIFN-β mediates tumor cell death in GL261 brain tumors.

(A) GL261 cells (5.0 ×10^4 cells) were implanted into the striatum of C57BL/6 mice and 12 days later, exo-AAV9–5NF-mIFN-b was injected i.v. and survival analysis performed. **(B)** GL261 cells (2.0 ×10^4 cells) were implanted into the striatum of C57BL/6 mice and 7 days later, exo-AAV9–5NF-mIFN-b was injected i.v. and survival analysis performed. H&E sections show small foci of necrosis, surrounded by viable tumor in the mIFN-B treated tumors, while the control group shows only scattered apoptotic cells and cystic change. Scale bar in high-magnification images is 100 μm.

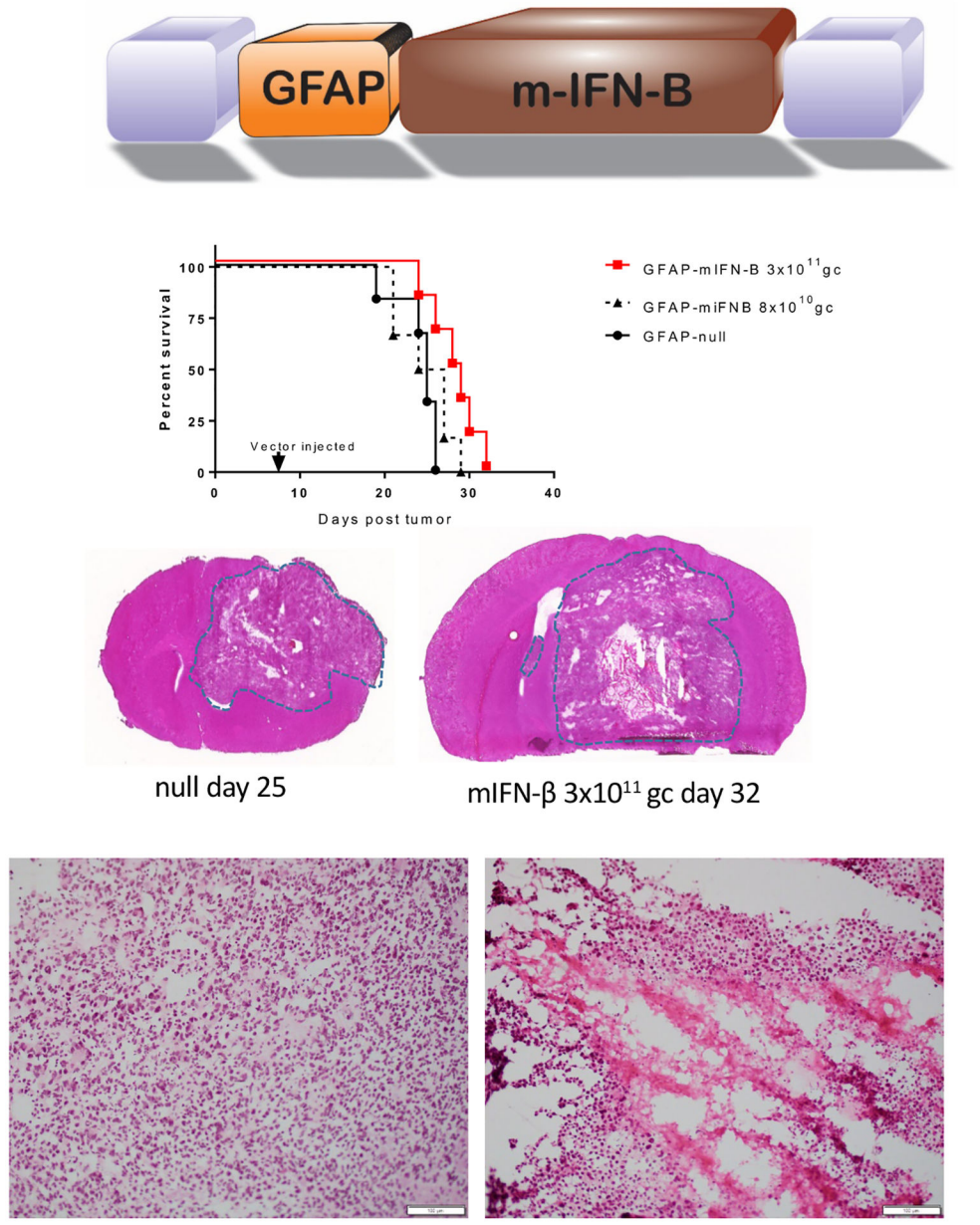

Figure 6. Systemically injected exo-AAV9-GFAP-mIFN-β increases survival.

GL261 cells (2.0 ×10^4 cells) were implanted into the striatum of C57BL/6 mice and 7 days later, exo-AAV9-GFAP-mIFN-b (two doses tested) or exo-AAV9-GFAP-null was injected i.v. and survival analysis performed. Significant (p=0.02) enhancement of survival was observed in the group treated with the higher dose of exo-AAV9-GFAP- mIFN-b compared to the control group. H&E sections show large areas of necrosis (50% of the tumor) surrounded by a rim of viable tumor in the treated tumors, while control tumors (GFAP null) show no evidence of confluent necrosis. Scale bar in high-magnification images is 100 μm.